A morphometric analysis of auditory brain regions in congenitally deaf adults

Karen Emmorey*†, John S. Allen‡, Joel Bruss‡, Natalie Schenker§, and Hanna Damasio*‡

*Laboratory for Cognitive Neuroscience, The Salk Institute for Biological Studies, 10010 North Torrey Pines Road, La Jolla, CA 92037; ‡Department of Neurology, University of Iowa, 2155 Roy Carver Pavillion, Iowa City, IA 52242; and §Department of Anthropology, University of California at San Diego, 9500 Gilman Drive, La Jolla, CA 92093

We investigated whether variation in auditory experience in humans during development alters the macroscopic neuroanatomy of primary or auditory association cortices. Volumetric analyses were based on MRI data from 25 congenitally deaf subjects and 25 hearing subjects, all right-handed. The groups were matched for gender and age. Gray and white matter volumes were determined for the temporal lobe, superior temporal gyrus, Heschl's gyrus (HG), and the planum temporale. Deaf and hearing subjects did not differ in the total volume or the gray matter volume of HG, which suggests that auditory deafferentation does not lead to cell loss within primary auditory cortex in humans. However, deaf subjects had significantly larger gray matter–white matter ratios than hearing subjects in HG, with deaf subjects exhibiting significantly less white matter in both left and right HG. Deaf subjects also had higher gray matter–white matter ratios in the rest of the superior temporal gyrus, but this pattern was not observed for the temporal lobe as a whole. These findings suggest that auditory deprivation from birth results in less myelination and/or fewer fibers projecting to and from auditory cortices. Finally, the volumes of planum temporale and HG were significantly larger in the left hemisphere for both groups, suggesting that leftward asymmetries within "auditory" cortices do not arise from experience with auditory processing.

The study of congenitally deaf adults provides a unique opportunity to investigate potential changes in neural organization and structure resulting from sensory deprivation. Animal studies have shown that congenital deafness produces degenerative changes in the central auditory pathway (1, 2). Degeneration in the central auditory system subsequent to profound hearing loss has also been reported in humans. For example, Moore and colleagues (3) observed cell size reductions in the cochlear nucleus of profoundly deaf adults. However, it is unclear whether auditory deprivation from birth results in degeneration of primary auditory cortex in either animals or humans. The pattern of subcortical projections to primary auditory cortex in congenitally deaf cats is similar to that of normally hearing cats (4, 5), suggesting that cortical auditory regions may continue to receive input from subcortical regions and might not exhibit degeneration. However, functional deficits are observed in synaptic activity and organization within auditory cortex (6), suggesting the possibility of variation in the structure of auditory cortex as a consequence of congenital deafness.

We investigated whether congenital and profound hearing loss in humans results in reduced volume and/or altered morphology of cortical brain regions involved in auditory processing. Specifically, we investigated whether lack of auditory input from birth affects gray matter (GM) and white matter (WM) volumes within primary auditory cortex [defined as the transverse gyrus of Heschl (7)], within auditory association cortex in the planum temporale (PT), or in the superior temporal gyrus (STG) as a whole. In addition, we examined possible interhemispheric anatomical differences for each of these structures to determine whether the leftward asymmetries observed in Heschl's gyrus

(HG) (8) and the PT (9) might be absent or reduced in deaf individuals who have no experience with auditory speech processing.

Previous investigations have found evidence suggesting use-dependent structural plasticity within both HG and the PT. For example, professional musicians with extensive early exposure to music show larger GM volumes within HG than nonmusicians (10). Musicians with perfect pitch also exhibit a larger leftward PT asymmetry than nonmusicians (11, 12). If such structural variation arises at least in part from the nature of auditory experience for musicians, it is reasonable to hypothesize that a complete lack of auditory input during development might lead to significant anatomical differences within HG and/or PT for deaf adults compared with normally hearing adults.

On the other hand, recent neuroimaging studies indicate that deaf adults who are native users of a signed language show activation of auditory brain regions in response to visual input. Using positron emission tomography, Petitto et al. (13) report bilateral activation in the PT when deaf native signers view individual signs or pseudosigns. Several functional MRI studies indicate activation in STG and PT when deaf adults view signed sentences (14, 15). MacSweeney et al. (15) further report that deaf signers demonstrate significantly greater activation in left STG than hearing native signers, suggesting that left auditory regions may be predisposed to processing speech, but in the absence of auditory input this region may be recruited for visual processing. Finally, Finney et al. (16) report activation in right auditory cortex when deaf signers view nonlinguistic visual stimuli (moving dot patterns). Together, these neuroimaging results indicate that auditory brain areas are functional in deaf adults exposed to sign language from birth, and therefore these areas may be less likely to degenerate in this population.

To address these issues, we undertook a volumetric investigation of auditory brain regions in congenitally deaf adults who were exposed to American Sign Language from birth. This study was designed to determine whether and how auditory deafferentation impacts the size and structure of auditory brain regions, and whether asymmetries within these regions arise in the absence of auditory input from birth but in the presence of an accessible visual–spatial language.

Methods

Subjects. Subjects were 25 congenitally deaf individuals (14 women and 11 men, average age 23.8 years, SD 4.1, range 19–38) and 25 hearing individuals (14 women and 11 men, average age 28.5 years, SD 5.4, range 22–39). All were right-handed, with scores on the Oldfield–Geschwind Handedness Inventory of >+90 (maximum right-handed score +100). Hearing and deaf subjects were all healthy with no history of neurological or

NEUROSCIENCE

psychiatric illness. Twenty-one deaf subjects exhibited profound hearing loss (>90 dB in the better ear), three subjects had severe hearing loss (>75 dB in the better ear), and one subject had moderately severe hearing loss (>55 dB in the better ear). Data on early hearing aid use were available from 17 deaf subjects. None used a hearing aid consistently before age 2. Eleven were required to wear hearing aids at school, but only two also wore their hearing aids at home, and six subjects did not wear hearing aids at school or at home. All deaf subjects were congenitally deaf and were born to deaf parents. American Sign Language (ASL) was the first and primary language of all of the deaf subjects. The hearing subjects were monolingual English speakers with no history of hearing disorder. All subjects gave informed consent in accordance with institutional and federal rules. Hearing subjects for this study were drawn from a pool of >240 normal volunteers who had MRI scans done in conjunction with functional imaging projects. The criteria for selection were the best age and gender match.

MR Image Acquisition. Thin-cut MR images were obtained in a GE Signa scanner operating at 1.5 T by using the following protocol: spoiled GRASS, flip angle 30° repetition time 24 ms, echo time 7 ms, number of excitations 1, acquisition matrix 256 × 192, field of view 24 cm. We obtained 124 contiguous coronal slices of 1.5 or 1.6 mm thickness and with interpixel distance of 0.94 mm. Three individual 1NEX SPGR datasets were obtained for each subject during each imaging session. These were coregistered and averaged post hoc by using AIR 3.03 (http://dns1.bmap.ucla.edu:16080/AIR3; refs. 17 and 18).

MR image analysis [3D reconstructions, volume determinations from regions of interest (ROIs)] were conducted by using BRAINVOX (19), an interactive family of programs designed to reconstruct, segment, and measure brains from MR-acquired images. An automated program, extensively validated against human experts (20), was used to segment the images into the three primary tissue types (white matter, gray matter, cerebrospinal fluid). Before tracing ROIs, brains were realigned (but *not* resized) along a plane running through the anterior and posterior commissures (i.e., the AC-PC line); this ensured that coronal slices in all subjects were perpendicular to a uniformly and anatomically defined axis of the brain.

ROIs. ROIs were traced by hand on contiguous coronal slices of the brain. Anatomical landmarks were identified and marked on the surface of 3D reconstructions of the two hemispheres and on a bilateral reconstruction of the brain from which the frontoparietal operculum had been removed, exposing the superior surfaces of the temporal lobes. The parcellation of the cerebrum and the temporal lobe was based on a scheme modified from (refs. 21 and 22; also see ref. 23), with additional consultation of several anatomical texts (including refs. 24–26). GM and WM volumes for the following ROIs are reported here: temporal lobe, STG, HG, and PT (see ref. 23, page 346, for tracing conventions used in this study).

Parcellation of the temporal lobe from the rest of the cerebrum is described in detail in ref. 23 (also see Figs. 3 and 4, which are published as supporting information on the PNAS web site, www.pnas.org). To define the superior boundary of the temporal lobe, the Sylvian fissure (SF) is followed to its most posterior extension. In cases where the SF splits into two branches, the branch that extends most posteriorly is followed (this is almost always the superior branch). The superoposterior boundary of the temporal lobe is defined by a line drawn on the lateral surface of the hemisphere, which connects the end of the SF to a plane that separates the occipital lobe from the rest of the cerebrum (Fig. 4); the inferoposterior boundary is defined by this occipital plane (see ref. 23 for a detailed description). The temporal pole (volume not reported here) is limited posteriorly by a plane that
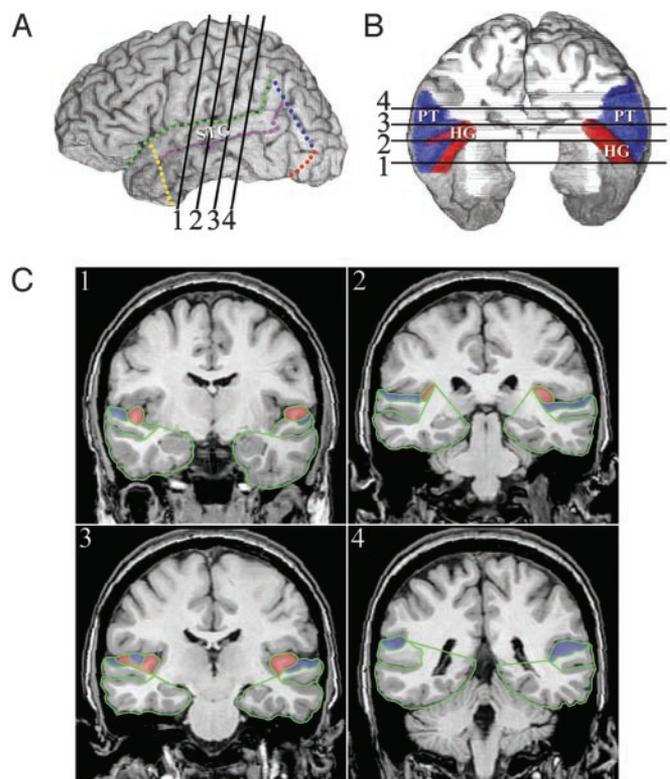

Fig. 1. Parcellation of HG and the PT. The position of the STG is shown in a lateral view of the left hemisphere in *A*. In *B*, a superior view of the temporal lobe (after removing the frontoparietal operculum) shows the relative positions of HG (red) and PT (blue) on the superior surface of STG. In the right hemisphere of this subject, Heschl's sulcus (the posterior boundary of HG) is discontinuous. Coronal slices (*C1–C4*) illustrate tracing of HG (red) and PT (blue) ROIs; positions of the coronal slices are indicated by the dark lines (1–4) in *A* and *B*.

includes the following three points (Fig. 3): On the lateral side of the hemisphere, point 1 is defined as the intersection between the SF and the horizontal and vertical branches of the SF, and point 2 is the most inferior point of the temporal lobe. Point 3 is defined on the first coronal slice (going from anterior to posterior) in which a WM connection is visible in the frontotemporal stem. On this slice, point 3 is placed on the mesial surface of the hemisphere at the level of the most inferior extension of the circular sulcus. The STG is limited superiorly by the SF and inferiorly by the superior temporal sulcus. Its anterior boundary is the temporal pole cut, and its posterior boundary is the posterior edge of the temporal lobe. If the superior temporal sulcus splits posteriorly into inferior and superior branches, the superior branch is followed [i.e., the branch that extends into the parietal lobe as the angular sulcus (24)].

HG is defined anteriorly by the first transverse sulcus of the temporal lobe and posteriorly by Heschl's sulcus (22). HG is the best macroscopic landmark for primary auditory cortex, even though the correspondence is not perfect (27). If there were two complete Heschl's sulci (i.e., Heschl's sulcus and a second transverse sulcus) defining two gyri, then the anterior gyrus was used. If Heschl's sulcus was discontinuous, a straight line was drawn connecting the anterior end of the posterior section to the posterior end of the anterior section, and the total length of the linked sulci was used as the posterior boundary of HG (Fig. 1). While marking landmarks, the anatomy of HG was checked repeatedly by simultaneously viewing the structure from different 2D orientations. In coronal slices, the lateral boundary of HG is formed by Heschl's sulcus. The mesial boundary, following

Table 1. Volumes (mm³) of brain sectors, GW ratios, and statistical comparisons of deaf and hearing subjects (effect sizes, *t* test *P* value, and univariate ANOVA *P* value)

Sector	Tissue	Deaf mean (SD)	Hearing mean (SD)	Mean difference (95% CI)	Effect size	*t* test *P* value	ANOVA *P* value*
Left temporal lobe	GM	76,061 (8,933)	73,714 (10,041)	2,347 (−3,057–7,752)	0.25	ns	na
	WM	40,808 (5,760)	39,714 (6,660)	1,094 (−2,447–4,635)	0.18	ns	na
	Total	116,869 (14,261)	113,427 (16,328)	3,441 (−5,276–12,159)	0.23	ns	na
	GW ratio	1.87 (0.13)	1.87 (0.12)	0.01 (−0.07–0.08)	0.05	ns	na
Right temporal lobe	GM	76,186 (9,170)	73,716 (11,000)	2,470 (−3,289–8,228)	0.24	ns	na
	WM	40,911 (6,292)	39,996 (7,681)	915 (−3,078–4,908)	0.13	ns	na
	Total	117,097 (15,165)	113,712 (18,278)	3,384 (−6,166–12,935)	0.20	ns	na
	GW ratio	1.87 (0.12)	1.86 (0.15)	0.01 (−0.07–0.09)	0.08	ns	na
Left STG	GM	16,011 (2,835)	16,099 (3,599)	−88 (−1,930–1,755)	0.03	ns	ns
	WM	5,493 (1,056)	6,020 (1,417)	−527 (−1,237–183)	0.42	ns	0.001
	Total	21,504 (3,765)	20,588 (4,426)	−615 (−3,109–1,879)	0.14	ns	0.039
	GW ratio	2.95 (0.33)	2.69 (0.25)	0.26 (0.9–0.43)	0.82	0.003	0.003
Right STG	GM	15,227 (2,838)	13,811 (2,987)	1,416 (−241–3,072)	0.48	ns	ns
	WM	6,809 (1,538)	6,777 (1,498)	429 (−832–895)	0.02	ns	ns
	Total	22,035 (4,279)	20,588 (4,426)	1,447 (−1,029–3,923)	0.33	ns	ns
	GW ratio	2.27 (0.23)	2.04 (0.15)	0.22 (0.11–0.33)	1.01	0.000	0.000
Left HG	GM	1,901 (561)	1,724 (398)	177 (−99–454)	0.36	ns	ns
	WM	554 (180)	640 (193)	−86 (−192–20)	0.45	ns	0.029
	Total	2,455 (722)	2,364 (565)	91 (−277–460)	0.14	ns	ns
	GW ratio	3.50 (0.56)	2.78 (0.52)	0.71 (0.41–1.02)	1.11	0.000	0.000
Right HG	GM	1,597 (381)	1,485 (420)	113 (−116–341)	0.28	ns	ns
	WM	542 (164)	636 (168)	−93 (47–−188)	0.54	0.053	0.012
	Total	2,140 (519)	2,120 (565)	19 (−289–328)	0.04	ns	ns
	GW ratio	3.05 (0.56)	2.35 (0.41)	0.69 (0.41–0.97)	1.15	0.000	0.000
Left PT	GM	3,479 (1,197)	3,059 (1,083)	421 (−228–1,070)	0.37	ns	ns
Right PT	GM	2,816 (754)	2,336 (748)	480 (53–907)	0.61	0.028	0.023
Left STG-minus-HG	GM	14,110 (2,464)	14,375 (3,410)	−265 (−1,957–1,427)	0.09	ns	ns
	WM	4,939 (988)	5,380 (1,337)	−441 (−1,110–227)	0.37	ns	0.005
	Total	19,049 (3,324)	19,755 (4,660)	−706 (−3,008–1,595)	0.18	ns	0.032
	GW ratio	2.90 (0.36)	2.69 (0.26)	0.21 (.03–.39)	0.65	0.020	0.021
Right STG-minus-HG	GM	13,629 (2,622)	12,326 (2,714)	1,303 (−215–2,820)	0.48	ns	ns
	WM	6,266 (1,450)	6,142 (1,387)	125 (−682–932)	0.09	ns	ns
	Total	19,895 (3,979)	18,468 (4,048)	1,428 (−855–3,710)	0.35	ns	ns
	GW ratio	2.21 (0.22)	2.01 (0.15)	0.19 (0.08–0.30)	0.90	0.001	0.000

CI, confidence interval; ns, not significant; na, not applicable.
*Univariate analysis of variance, with temporal lobe volume (gray, white, or total, as appropriate) as covariable.

ref. 8, is the ''meeting of gyrus and stem,'' which is usually marked by an indentation at the base of HG on its mesial surface.

The PT was defined as the cortex of the superior surface of the STG (excluding HG), starting anteriorly with the first coronal slice in which HG appears, and continuing posteriorly until the end of the SF. In each coronal slice, the planum was traced to include all of the cortex from (and including) the lateral wall of Heschl's sulcus (where it was present), across the superior surface of the STG, to the lateral edge of the SF. Posterior to HG, the planum is defined as the cortex of the superior surface of the STG. The GM of intervening sulci on the surface of the STG were included in the PT. Because we followed the planum until the end of the SF, in many cases our PT ROI includes the so-called ''planum parietale,'' which has been defined as the posterior ascending portion of the SF (28).

Reliability. For the deaf subjects, all ROIs were traced by two tracers (J.B. and N.S.); their work was checked by two other investigators (J.S.A. and H.D.). For the hearing subjects, all ROIs were traced by J.B. and checked by J.S.A. and H.D., and a subset of 10 hearing brains were also traced by N.S. Tracing reliability for STG, HG, and PT was checked by using the 25 deaf brains and the 10 hearing brains traced by J.B. and N.S. The results were as follows (Pearson's *r*, *P* < 0.01 for all): left STG,

GM 0.95/WM 0.94; right STG, GM 0.93/WM 0.91; left HG, GM 0.93/WM 0.90; right HG, GM 0.87/WM 0.74; left PT, 0.92; right PT, 0.87. There was no statistical difference in the correlations for the hearing and deaf brains for either the HG or PT tracings.

Data Analysis. Statistical analyses were performed by using SPSS 9.0.0 for Windows (SPSS, Chicago). Independent samples *t* tests and univariate ANOVA were used to compare means. Effect sizes (absolute difference of means/pooled standard deviation) and 95% confidence intervals were used to calculate the magnitude of volume differences between deaf and hearing subjects. Effect sizes of 0.20, 0.50, and >0.80 were considered small, medium, and large, respectively (29). Hemispheric asymmetries were examined with pairwise *t* tests and a conventional asymmetry index ($[L − R]/[[L + R]/2]$).

Results

Volumetric and gray–white (GW) ratio results comparing deaf and hearing subjects are presented in Table 1 (data from individual subjects are presented in Tables 3 and 4, which are published as supporting information on the PNAS web site). For the ANOVA analyses, temporal lobe volume was a covariable in comparing deaf and hearing means of smaller temporal lobe sectors; thus, the ANOVA *P* values provide a size-corrected
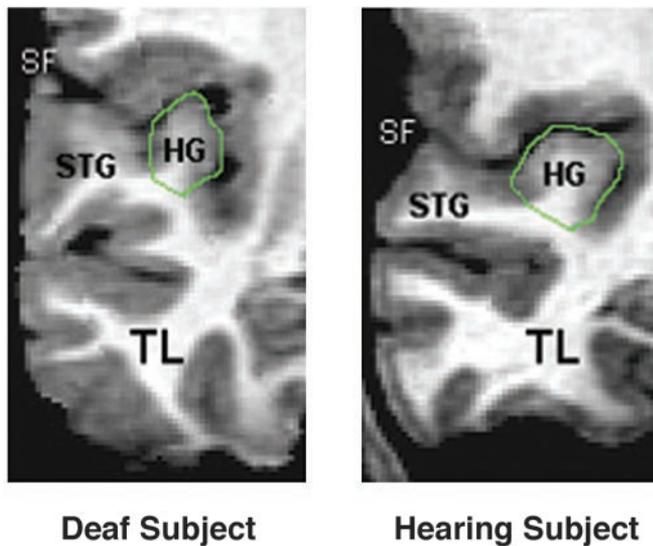
Fig. 2. Comparison of right Heschl's gyri (HG) in a deaf subject and a hearing subject demonstrating reduced WM volume in the deaf subject. Coronal slices were taken at the anteroposterior midpoint of each HG. TL, temporal lobe.

comparison between the two groups. Temporal lobe volumes from the appropriate hemisphere and for the appropriate tissue type were used as the covariables (e.g., for left HG GM, left temporal lobe GM volume was used as the covariable).

Overall temporal lobe volumes were very similar in deaf and hearing subjects. Effect sizes indicated that the GW ratio was somewhat higher in deaf subjects, although not significantly so. In the STG, the GW ratio was significantly higher in the deaf subjects compared with the hearing subjects. This was primarily a result of the deaf subjects having significantly less WM in the STG than hearing subjects in the left hemisphere. In the right STG, the higher GW ratio in deaf subjects was a product of both greater GM volume and smaller WM volume.

The volumetric results from HG indicated that WM volume in this part of the STG was significantly reduced in deaf subjects compared with hearing subjects (Fig. 2), and thus the GW ratio was significantly higher in the deaf subjects. There were no significant differences in HG GM volume between hearing and deaf subjects.

HG comprises ≈10–11% of the STG. Is the WM reduction in deaf subjects seen in the left STG due only to the WM reduction in HG? Or is the difference due to a more general WM reduction in the STG? To examine this issue, we compared the GW ratios of the STG with the exclusion of HG (STG-minus-HG) and found that GW ratios were still significantly higher in deaf

subjects. The greater GW ratio in the deaf subjects' left STG-minus-HG is clearly due to significantly smaller WM volume. On the right side, the deaf GM STG-minus HG volume is substantially larger in deaf subjects, whereas the WM volume is about the same, resulting in the higher GW ratio. These results suggest that there may be WM reductions in deaf subjects in the STG outside of HG, although it was not as pronounced as the WM reduction in HG.

The PT volume was somewhat larger in deaf subjects compared with hearing subjects. The difference reached statistical significance in the right hemisphere, but not in the left, although the effect size difference between the groups was substantial (Table 1). The PT comprised a larger proportion of the STG-minus-HG GM in deaf subjects compared with hearing subjects. In the left hemisphere, the difference was significant (*t* test, *P* = 0.024), with the planum comprising 24.2% (SD 5.4%) of the non-HG STG in deaf subjects, compared with 21.1% (SD 4.3%) in hearing subjects. In the right hemisphere, the difference approached significance (*P* = 0.066), with the deaf proportion at 20.7% (SD 3.9%) and the hearing proportion at 18.7% (SD 3.5%).

Asymmetry statistics are presented in Table 2. Both hearing and deaf subjects exhibited the expected and substantial leftward asymmetry in PT volume. Substantial leftward asymmetries were also seen in the GM of HG in both subject groups. Both hearing and deaf subjects had a substantial rightward asymmetry in WM volume of the STG, consistent with other volumetric STG studies (30). Significant differences in asymmetry between the two groups were found for two measures. First, STG GM volume in hearing subjects was substantially larger on the left, whereas in deaf subjects there was not a strong pattern of asymmetry in either direction. Second, the total volume of the STG was significantly larger in the left hemisphere of hearing subjects, whereas no such asymmetry can be found in deaf subjects.

Discussion

Our results show that in humans, auditory deprivation from birth results in a bilateral increase in GW ratios in primary auditory cortex (defined as HG), extending into auditory association cortex within the STG. The increase in GW ratios is largely due to a reduction in WM volume in deaf subjects, suggesting that auditory deafferentation results in less myelination, fewer fibers projecting to and from auditory cortices, or greater axonal pruning in the congenitally deaf. In humans with normal hearing, myelination of thalamic fibers projecting to auditory cortex begins around 1 year and continues until age 4, and overall axonal density only stabilizes between 11 and 12 years of age (31, 32). Increased myelination and axonal growth are accompanied by decreases in the response latency and amplitude of early auditory evoked potentials (P1 and N1) across the same developmental time span (33). Our findings suggest that the degree of

Table 2. Asymmetry statistics

Sector	Status	Asymmetry index (SD)			Pairwise *t* test *P* value			
		GM	WM	Total	GM	WM	Total	GW ratio
Temporal lobe	D	−0.001 (0.064)	−0.002 (0.099)	−0.001 (0.074)	ns	ns	ns	ns
	H	0.001 (0.077)	−0.003 (0.121)	−0.000 (0.092)	ns	ns	ns	ns
HG	D	0.159 (0.213)	0.018 (0.258)	0.125 (0.212)	0.000 (l > r)	ns	0.003 (l > r)	0.001 (l > r)
	H	0.158 (0.265)	−0.007 (0.290)	0.111 (0.259)	0.008 (l > r)	ns	0.045 (l > r)	0.000 (l > r)
STG	D	0.050 (0.137)*	−0.208 (0.171)	−0.022 (0.142)*	ns	0.000 (r > l)	ns	0.000 (l > r)
	H	0.149 (0.173)	−0.120 (0.182)	0.069 (0.173)	0.000 (l > r)	0.003 (r > l)	0.049 (l > r)	ns
PT	D	0.186 (0.189)			0.000 (l > r)			
	H	0.252 (0.342)	na	na	0.001 (l > r)	na	na	na

Asymmetry index = (L − R)/[(L + R)/2]. D, deaf; H, hearing; ns, not significant; na, not applicable; l, left; r, right.
*Difference between deaf and hearing subjects (*t* test) *P* < 0.05.

Emmorey *et al.*

myelination (or axonal growth) within auditory cortices may depend on sound input during development. Decreased WM volume was most pronounced within HG, suggesting that an experience-dependent growth of myelin (or of axonal connections) may be particularly pronounced in relation to primary auditory cortex.

Bavelier and Neville (34) hypothesize that sensory deprivation might lead to degeneration of long-range cortico-cortical connectivity. Falchier and colleagues (35) report the existence of a pathway from primary auditory cortex to the zone within primary visual cortex (V1) that supports peripheral vision in adult monkeys. Bavelier and Neville (ref. 34, page 447) hypothesize that "degeneration of this connection might reduce the interactions between auditory and visual projections in this convergence zone that mediates peripheral vision, allowing enhanced visual skills in the peripheral field, which have been noted in deaf individuals" (see, for example, ref. 36). Our finding of reduced WM volume within the auditory brain regions of congenitally deaf adults provides support for this hypothesis. Of course, reduced WM could also result from decreased projects from the thalamus or ipsilateral and/or contralateral auditory cortical areas.

According to our findings, lack of auditory experience from birth does not appear to alter the total volume of GM within primary auditory cortex. Although congenital deafness can lead to neuronal degeneration within subcortical auditory structures, such as the cochlear nucleus or inferior colliculus (2, 37), our results indicate that cell loss may well be absent within cortical auditory structures. Neurons within HG and auditory association cortex may not atrophy because these neurons may come to respond to nonauditory input. Responses to both tactile (38) and visual (16) input have been reported in auditory cortex of congenitally deaf individuals.

In contrast to our deaf subjects, the hearing subjects exhibited a leftward asymmetry for GM within STG and total STG volume. Previous studies with normally hearing control subjects have also reported a leftward asymmetry for STG volume (30, 39). The lack of asymmetry within STG for the deaf subjects may be due to the increased GM volume within right STG. GM volume did not differ between deaf and hearing subjects within left STG, but did differ within the right STG.

Somewhat surprisingly, neither hearing nor deaf subjects exhibited a significant WM asymmetry within HG. Previously, Penhune and colleagues (8) reported a leftward WM asymmetry in HG and attributed the asymmetry to enhanced left-hemisphere processing of temporal aspects of auditory stimuli, particularly rapidly changing speech signals. However, the fact that our deaf subjects exhibited a leftward WM asymmetry (although nonsignificant) casts some doubt on this interpretation of the WM asymmetry in primary auditory cortex.

Both subject groups exhibited a leftward GM asymmetry in HG and the PT. Leftward asymmetry in HG has been previously reported for normally hearing adults (22, 40, 41). Our results indicate that this leftward asymmetry is not likely to be related to experience with spoken language or to auditory processing in general. The leftward asymmetry in the PT was first reported by Geschwind and Levitsky (9) and has been replicated many times (see ref. 42 for a review). The PT asymmetry was originally thought to reflect left hemisphere dominance for language, particularly because the planum overlaps with Wernicke's area. However a leftward asymmetry has been reported in the PT of chimpanzees (43) and great apes (44), suggesting that the asymmetry may not be driven by linguistic processing. Our results further show that the leftward PT asymmetry is not driven by auditory experience during development.

In sum, this is the first study that we know of to report WM changes in human primary sensory cortical regions due to sensory deprivation from birth. The reduction in WM volume was not accompanied by a similar reduction in GM volume. This finding can be seen as consistent with reports of neural activity in auditory cortices for deaf individuals in response to nonauditory stimuli (13–16, 38). Finally, congenital deafness accompanied by life-long use of sign language does not seem to alter the leftward asymmetries found for HG (primary auditory cortex) or the PT.

1. Saada, A. A., Niparko, J. K. & Ryugo, D. K. (1996) *Brain Res.* **736,** 315–328.
2. Tierney, T. S., Russell, F. A. & Moore, D. R. (1997) *J. Comp. Neurol.* **378,** 295–306.
3. Moore, J. K., Niparko, J. K., Miller, M. R. & Linthicum, F. H. (1994) *Am. J. Otol.* **15,** 588–595.
4. Stanton, S. G. & Harrison, R. V. (2000) *J. Comp. Neurol.* **426,** 117–129.
5. Heid, S., Jahn-Siebert, T. K., Klinke, R., Hartmann, R. & Langner, G. (1997) *Hear. Res.* **110,** 191–199.
6. Kral, A., Hartmann, R., Tillein, J., Heid, S. & Klinke, R. (2000) *Cereb. Cortex* **10,** 714–726.
7. Galaburda, A. M. & Sanides, F. (1980) *J. Comp. Neurol.* **190,** 597–610.
8. Penhune, V. B., Zatorre, R. J., MacDonald, J. D. & Evans, A. C. (1996) *Cereb. Cortex* **6,** 661–672.
9. Geschwind, N. & Levitsky, W. (1968) *Science* **161,** 186–187.
10. Schneider, P., Scherg, M., Günter Dosch, H., Specht, H. J., Gutschalk, A. & Rupp, A. (2002) *Nat. Neurosci.* **5,** 688–694.
11. Schlaug, G., Jancke, L., Huang, Y. & Steinmetz, H. (1995) *Science* **267,** 699–701.
12. Keenan, J. P., Thangaraj, V., Halpern, A. R. & Schlaug, G. (2001) *NeuroImage* **14,** 1402–1408.
13. Petitto, L. A., Zatorre, R. J., Gauna, K., Nikelski, E. J., Dostie, D. & Evans, A. (2000) *Proc. Natl. Acad. Sci. USA* **97,** 13961–13966.
14. Neville, H., Bavelier, D., Corina, D., Rauschecker, J., Karni, A., Lalwani, A., Braun, A., Clark, V., Jezzard, P. & Turner, R. (1998). *Proc. Natl. Acad. Sci. USA* **95,** 922–929.
15. MacSweeney, M., Woll, B., Campbell, R., McGuire, P. K., David, A. S., Williamis, S. C., Suckling, J., Calvert, G. A. & Brammer, M. J. (2002) *Brain* **125,** 1583–1593.
16. Finney, E. M., Fine, I. & Dobkins, K. R. (2001) *Nat. Neurosci.* **4,** 1171–1173.
17. Woods, R., Cherry, S. R. & Mazziotta, J. C. (1992) *J. Comput. Assist. Tomogr.* **16,** 620–633.
18. Holmes, C. J., Hoge, R., Collins, L., Woods, R. P., Evans, A. C. & Toga, A. W. (1998) *J. Comput. Assist. Tomogr.* **22,** 244–333.
19. Frank, R. J., Damasio, H. & Grabowski, T. J. (1997) *NeuroImage* **5,** 13–30.
20. Grabowski, T. J., Frank, R. J., Szumski, N. R., Brown, C. K. & Damasio, H. (2000) *NeuroImage* **12,** 640–656.
21. Rademacher, J., Galaburda, A. M., Kennedy, D. N., Filipek, P. A. & Caviness, V. S. (1992) *J. Cognit. Neurosci.* **4,** 352–374.
22. Rademacher, J., Caviness, V. S., Steinmetz, H. & Galaburda, A. M. (1993) *Cereb. Cortex* **3,** 313–329.
23. Allen, J. S., Damasio, H. & Grabowski, T. J. (2002) *Am. J. Phys. Anthropol.* **118,** 341–358.
24. Ono, M., Kubik, S. & Abernathey, C. D. (1990) *Atlas of the Cerebral Sulci* (Thieme, New York).
25. Damasio, H. (1995) *Human Brain Anatomy in Computerized Images* (Oxford Univ. Press, New York).
26. Duvernoy, H. (1991) *The Human Brain* (Springer, New York).
27. Rademacher, J., Morosan, P., Schormann, T., Schleicher, A., Werner, C., Freund, H.-J. & Zilles, K. (2001) *NeuroImage* **13,** 669–683.
28. Jäncke, L., Schlaug, G., Huang, Y. & Steinmetz, H. (1994) *NeuroReport* **5,** 1161–1163.
29. Welkowitz, J., Ewen, R. B. & Cohen, J. (1982) *Introductory Statistics for the Behavioral Sciences* (Harcourt Brace Jovanovich, San Diego).
30. De Bellis, M. D., Keshavan, M. S., Frustaci, K., Shifflett, H., Iyengar, S., Beers, S. & Hall, J. (2002) *Biol. Psychiatry* **51,** 544–552.
31. Moore, D. R. (2002) *Br. Med. Bull.* **63,** 171–181.
32. Moore, J. K. & Guan, Y. L. (2001) *J. Assoc. Res. Otolaryngol.* **2,** 297–311.
33. Ponton, C. W., Eggermont, J. J., Kwong, B. & Don, M. (2000) *Clin. Neurophysiol.* **111,** 220–236.
34. Bavelier, D. & Neville, H. (2002) *Nat. Rev. Neurosci.* **3,** 443–452.

NEUROSCIENCE

35. Falchier, A., Clavagnier, S., Barone, P. & Kennedy, H. (2002) *J. Neurosci.* **22,** 5749–5759.

36. Bavelier, D., Tomann, A., Hutton, C., Mitchell, T., Liu, G., Corina, D. & Neville, H. (2000). *J. Neurosci.* **20,** RC93.

37. Nishiyama, N., Hardie, N. A. & Shepherd, R. K. (2000) *Hear. Res.* **140,** 18–22.

38. Levänen, S., Jousmäki, V. & Hari, R. (1998) *Curr. Biol.* **8,** 869–872.

39. Rajarethinam, R. P., DeQuardo, J. R., Nalepa, R. & Tandon, R. (2000) *Schizophr. Res.* **41,** 303–312.

40. Dickey, C. C., McCarley, R. W., Voglmaier, M. M., Niznikiewicz, M. A., Hirayasu, Y., Fraone, S., Seidman, L. J. & Shenton, M. E. (2002) *Am. J. Psychiatry* **159,** 1521–1527.

41. Good, C. D., Johnsrude, I., Ashburner, J., Henson, R. N. A., Friston, K. J. & Frackowiak, R. S. J. (2001) *NeuroImage* **14,** 685–700.

42. Shapleske, J., Rossell, S. L., Woodruff, P. W. R. & David, A. S. (1999) *Brain Res. Brain Res. Rev.* **29,** 26–49.

43. Gannon, P., Holloway, R. L., Broadfield, D. C. & Braun, A. R. (1998) *Science* **279,** 220–222.

44. Hopkins, W., Marino, L., Rilling, J. & MacGregor, L. (1998) *NeuroReport* **9,** 2913–2918.